Palaeontology
The Palaeontological Association
www.palass.org
[Palaeontology, 2023, e12676]

Bridging the extant and fossil record of planktonic foraminifera: implications for the *Globigerina* lineage

by ALESSIO FABBRINI[1,*], MATTIA GRECO[2], FRANCESCO IACOVIELLO[3], MICHAL KUCERA[4], THOMAS H.G. EZARD[5] *and* BRIDGET S. WADE[1]

[1]Department of Earth Sciences, University College of London, Gower Street, London WC1E 6BT, UK; a.fabbrini@ucl.ac.uk, b.wade@ucl.ac.uk
[2]Institute of Oceanology, Polish Academy of Sciences, 81-712 Sopot, Poland; mgreco@iopan.pl
[3]Department of Chemical Engineering, University College of London, Gower Street, London WC1E 6BT, UK; f.iacoviello@ucl.ac.uk
[4]MARUM – Center for Marine Environmental Sciences, University of Bremen, Leobener Str. 8, D-28359 Bremen, Germany; mkucera@marum.de
[5]School of Ocean and Earth Science, University of Southampton, European Way, Southampton SO14 3ZH, UK; t.ezard@ston.ac.uk
*Corresponding author

Typescript received 24 January 2023; accepted in revised form 27 July 2023

Abstract: We conducted a morphometric study and wall texture analysis on extant and fossil specimens of the planktonic foraminifera *Globigerina falconensis* plexus. Our global data reveal morphological inconsistencies between fossil and extant populations. Our results are significant as *G. falconensis* is widely used in palaeoceanographic studies in conjunction with its sister taxon *G. bulloides*. Morphologically these two species are similar, with the main difference being the distinctive apertural lip present in *G. falconensis*. We selected cores covering the entire stratigraphic range of *G. falconensis*, from the early Miocene to current day, spanning sites from high latitudes in the North Atlantic Ocean and the southern Indian Ocean to sites in equatorial regions. The morphology found in the modern ocean is not consistent with the Miocene holotype of *Globigerina falconensis* Blow described from lower Miocene sediments in Venezuela. A more lobate morphology evolved in the late Miocene, thus, a new name is required for this morphotype, coexisting in the modern oceans with *G. falconensis s.s.* We thus describe the new morphospecies, *G. neofalconensis* for the more lobate forms which evolved in the late Miocene and inhabit the modern oceans. Additionally, we report a pseudocancellate wall texture present in the *G. falconensis* plexus. We use the molecular sequences from the PR^2 database to explore the generic attribution of the *G. falconensis* lineage, confirming its close relationship with *G. bulloides* and its retention in the genus *Globigerina*.

Key words: planktonic foraminifera, extant, *Globigerina*, taxonomy, genetic, morphometric.

PLANKTONIC foraminifera are widely used in biostratigraphy, palaeoceanography and evolutionary studies as indicators of time and past ocean conditions and chemistry. These applications require a robust identification of species, since without clear taxonomic concepts, information on diversity and palaeoecology will be misinterpreted. Taxonomy is based on types, which capture the essence of a species, but not the range of its variability (Scott 2011) and especially not through time. This often leads to conflicting classifications and in some cases, the established concept of a morphospecies may even become disconnected from the type specimen (Fabbrini *et al.* 2021). For example, this could occur when a species is associated with a type that has been considered in isolation of the variability in the population from which it is derived (Scott 2011), as may happen when scanning electron micrograph (SEM) images of the type specimen are unavailable. Every situation where the taxon concept is not consistent with the type causes taxonomic instability (Wade *et al.* 2018; Fabbrini *et al.* 2021). In organisms that have a rich fossil record, this problem is epitomized when names of living taxa are based on fossil types. It is extremely important to understand the living plankton and to put the modern taxa in the context of their taxonomic history and fossil record (Morard *et al.* 2022). A taxonomic review of the living planktonic foraminifera was undertaken by Brummer & Kučera (2022), in which they recognized 50 extant species living in the modern oceans.

Planktonic foraminifera are an example of a group in which the palaeontological and biological classifications are interwoven, and two extant species have fossil types: *Globoquadrina conglomerata* and *Globigerina falconensis*. Brummer & Kučera (2022) highlighted the issues that arise when extant species are described from sediments rather than from the plankton, and the need for a thorough assessment to demonstrate the equivalency of fossil types and their living species. This is the case for the

doi: 10.1111/pala.12676

living taxon *G. falconensis* (Fig. 1), a long ranging species described by Blow (1959) from the Burdigalian (lower Miocene) sediments of Falcón (Venezuela).

The genus *Globigerina* is typified by trochospiral coiling, globular chambers, a single umbilical aperture and spinose wall consisting of small (<0.9 μm in diameter) pores and spine collars, termed *bulloides*-type by Hemleben & Olsson (2006). It ranges from the middle Eocene (Zone E9) to today. There are several fossil genera sharing morphological similarities with *Globigerina*, but they all lack the characteristic *bulloides*-type wall; for example, *Subbotina* and *Globoturborotalita*, which have a cancellate wall texture (Hemleben & Olsson 2006). The current classification of the genus *Globigerina* comprises two extant species, *G. bulloides* and *G. falconensis* (Fig. 1), which are common in modern assemblages from many marine environments. The two species are morphologically similar, both possessing four globular chambers in the final whorl, increasing slowly in size, with an umbilical aperture. The chief distinction between *G. falconensis* and *G. bulloides* is the characteristic apertural lip present in *G. falconensis*. The two taxa show some ecological differences, and for this reason they are commonly used in palaeoclimatic studies (Malmgren & Kennett 1978; Naidu & Malmgren 1996; Li *et al.* 2001; Xu *et al.* 2005). *Globigerina bulloides* is most abundant at higher latitudes and in eutrophic areas, such as upwelling localities. The extant *G. falconensis* has a more cosmopolitan range (Siccha & Kucera 2017) and is more abundant in mid-latitudes, and in monsoonal and upwelling conditions (Malmgren & Kennett 1978; Naidu & Malmgren 1996; Li *et al.* 2001; Xu *et al.* 2005). Both *G. falconensis* and *G. bulloides* inhabit the mixed-layer (Sousa *et al.* 2014; among others). The correct identification of *G. falconensis* is then crucial to understand the extent and origin of biodiversity in living planktonic foraminifera, to interpret the evolution of the group, and to constrain its palaeoecological applications. *Globigerina falconensis* has been reported frequently in the fossil record, and its lowest occurrence has been used to calibrate molecular clocks in genetic studies (André *et al.* 2014; among others).

Despite clear evidence for morphological distinction, *G. falconensis* has been misidentified or grouped with its sister taxon *G. bulloides* (Al-Sabouni *et al.* 2018; Fenton *et al.* 2018; Hsiang *et al.* 2019), and some authors have even questioned the validity of *G. falconensis* (Bé 1968; Kennett 1969). To solve this issue, morphological analyses were conducted in order to define the key features distinguishing *G. falconensis* from *G. bulloides* (Malmgren & Kennett 1977), but that study neglected the extensive analysis of fossil specimens. Therefore, we revisited the taxonomic concept of *G. falconensis* by sampling and analysing large populations of *G. falconensis* from multiple locations and throughout its stratigraphic record, from the early Miocene to the current day. Here we sought to establish whether there is consistency between fossil type and living forms of *G. falconensis* through the study of both fossil and extant populations, including the re-examination of the type material deposited at the Natural History Museum (London).

MATERIAL AND METHOD

For this study, ocean floor drilled cores from several DSDP, ODP and IODP sites have been used, respectively: DSDP Site 590, ODP Site 662, ODP Site 747, ODP Site 871, ODP Site 925, ODP Site 982, ODP Site 984, IODP Site U1482, IODP Site U1489, IODP Site U1490 and Meteor M32/2 (Fig. 2). We selected cores which covered

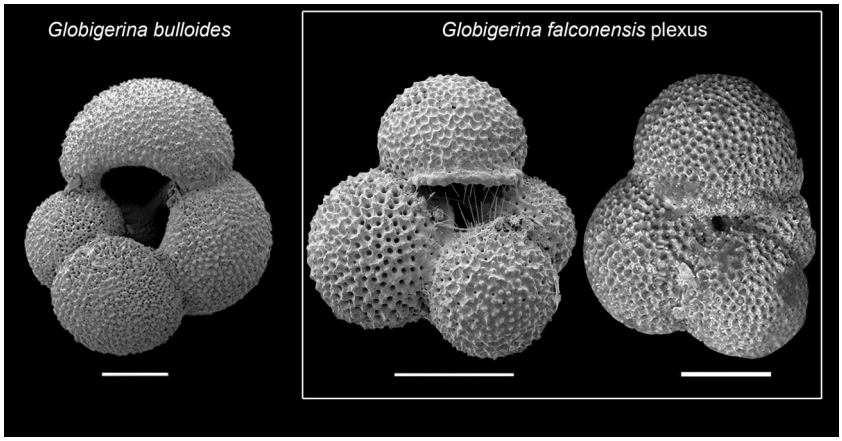

FIG. 1. SEM micrographs of modern specimens of *Globigerina bulloides*, *G. falconensis*, and the holotype of *G. falconensis* Blow, 1959, from the early Miocene. All scale bars represent 100 μm.

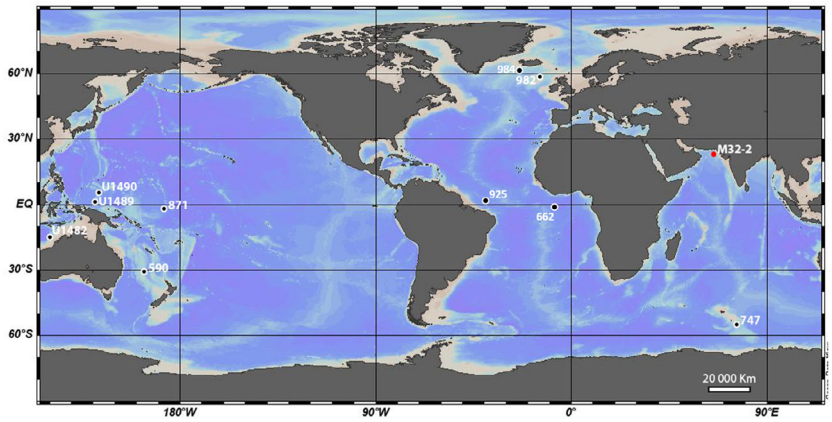

FIG. 2. Location of the studied sites. The DSDP, ODP and IODP sites are indicated in black; the Meteor site is shown in red. Map created using Ocean Data View (Schlitzer 2022).

the fossil range of *G. falconensis* globally and with good fossil preservation, spanning from two sites at high latitudes (ODP Site 982 in the North Atlantic Ocean and ODP Site 747 in the southern Indian Ocean) to two sites in equatorial regions (IODP Site U1489 and ODP Site 871), and the Meteor M32 in the subtropical Arabian Sea. ODP Site 925 is located in the western equatorial Atlantic, and constitutes a particularly relevant study area, since it is not far from the type locality of *G. falconensis* Blow, 1959, in Venezuela.

Micropalaeontological analysis

Sample preparation. All samples were prepared following the standard washing, drying and sieving procedures. First, the samples were pre-soaked in *c.* 150 mL of distillate water to disaggregate the sediments, and then washed with tap and distilled water, sieving the sediment through a 63 μm mesh. The residues were oven dried at 40°C. Different size fractions were obtained through 250 and 125 μm dry sieves for each sample. The samples from Meteor M32/2 (Recent from the Arabian Sea) were sieved in different size fractions: above 400, 400–315, 315–250, 250–200, 200–150, below 150 μm. Total population picking was conducted in order to characterize the assemblages. Microfossil specimens were examined under a continuous-zoom stereo microscope. Well preserved specimens and entire populations available of the *G. falconensis* plexus were picked and stored on microslides for further imaging and analysis. Species identification was based on the literature (Bolli 1957; Blow 1959, 1969; Kennett & Srinivasan 1983; Bolli *et al.* 1985; Spezzaferri 1994; Aze *et al.* 2011; Fox & Wade 2013; Wade *et al.* 2018) and the online archive Mikrotax (Huber *et al.* 2016).

Imaging. Unbroken specimens were selected for SEM imaging and further scanning. The selected specimens were stuck on metal stubs using double-sided sticky tape. The stubs were coated with gold and inspected using a Jeol JSM-6480LV high-performance, variable pressure analytical scanning electron microscope at the Department of Earth Sciences, University College London (UCL). Optical photographs were taken using an OLYMPUS DP73 multifocal camera mounted on an OLYMPUS SZX16 stereo microscope at the at the Department of Earth Sciences, UCL. The images were taken using a step of 15 μm and an average imaging time of 60 s per specimen. The images were then postprocessed using the software Stream Motion (Olympus).

Micro computed tomography. One specimen was selected for a high-resolution imaging using micro computed tomography (micro-CT). The three-dimensional microstructure of the selected specimen was studied using a ZEISS Xradia 620 Versa x-ray computed tomography microscope, located at the Electrochemical Innovation Lab (EIL), part of the Department of Chemical Engineering, UCL. The specimen was mounted as single specimen set up following a protocol modified after Coletti *et al.* (2018). The sample was scanned for a total of 60 min with a maximum resolution of 500 nm. In total, 1601 radiographs were acquired over a 360° sample rotation range with an exposure time of 25 s per radiograph. The sample was placed between the x-ray source and a 2 k × 2 k detector with a source-to-detector distance of 39.9 mm providing a voxel resolution of *c.* 500 nm using the 20× objective magnification in binning 1 mode. The instrument was operated at 80 kV and 7 W, employing a low energy filter to optimize transmission and contrast to noise ratio. The raw transmission images from micro-CT imaging experiment were reconstructed using a commercial image reconstruction

software package (Zeiss XMReconstructor, Carl Zeiss X-ray Microscopy Inc., Pleasanton CA), which employs a filtered back-projection algorithm. The reconstructed greyscale 3D image volumes were subsequently segmented using the Avizo 3D 2022.1 software package (ThermoFisher Scientific, Waltham MA). The surface was then generated and saved as an STL file.

Morphometry. All measurements for the morphometric study were conducted on the entire picked populations of *G. falconensis* plexus, using the software Image Pro, and ana QImaging RETIGA-2000R camera mounted on a light microscope at the Department of Earth Sciences, UCL. The following three parameters were selected and measured: area (A) (μm^2), diameter (D) (μm), roundness (R). This last parameter (roundness) was obtained from A and D, using Image Pro. All data were plotted using the statistical software PAST (Hammer *et al.* 2001).

Molecular analysis. To investigate the genetic evolution of the *G. falconensis* plexus, we accessed curated SSU rDNA sequences of the species *G. falconensis*, *Globoturborotalita rubescens*, *Globigerinoides tenellus*, *Globigerinoides elongatus*, *Globigerinoides conglobatus* and *Globigerinoides ruber albus* from the PR^2 database (https://pr2-database.org; Guillou *et al.* 2013) (Table 1) using the R package PR^2database in R v4.1.1 (R Core Team 2013; Vaulot 2022). To ensure that the resulting topology is not affected by long-branch attraction towards *G. bulloides* and the phylogenetic placement of *G. falconensis* emerges independently, we excluded on purpose *G. bulloides*. We set up the molecular clock analyses using the divergence between *Globoturborotalita rubescens* (as representative of the entire genus *Globoturborotalita*) and *Globigerinoides* at 23.8 Ma (Aurahs *et al.* 2011), and the first occurrence of *Globigerinoides conglobatus* (8–8.6 Ma in Aze *et al.* 2011), and *Globigerinoides tenellus* (2.5 Ma in Aze *et al.* 2011), which are all well-known data from the fossil record (Kucera & Schönfeld 2007).

We used a 'relaxed' clock model as implemented in BEAST v1.8.4 (Suchard *et al.* 2018). The model parameters were set using BEAUti v1.8.4. The distribution of the fixed node age prior was considered normal and the speciation rate was assumed constant under the Yule-Process. The generalized time reversible (GTR) model was selected as a substitution model. Markov-Chain Monte Carlo (MCMC) analyses were conducted for 10 000 000 generations, with a burn-in of 1000 generations and saving each 1000th generation. The maximum clade credibility tree with median node heights was calculated in TREEAnnotator v1.8.4 from the BEAST package, with a burn-in of 100 trees and a posterior probability limit of 0. The resulting tree was then imported into the R environment using the read.beast function from the treeio package (Wang *et al.* 2020). The tree was successively visualized using the R package ggtree (Yu *et al.* 2017) and a geological time scale was added using the R package deeptime (Gaerty 2022).

TABLE 1. Accession number of the SSU rDNA sequences extracted from the PR^2 database (Guillou *et al.* 2013) used for the molecular clock analysis (Fig. 6).

Accession no.	Genus	Species
KM194166	*Globigerina*	*falconensis*
MN384086	*Globoturborotalita*	*rubescens*
MN384073	*Globoturborotalita*	*rubescens*
Z69599	*Globigerinoides*	*ruber albus*
EU012486	*Globigerinoides*	*ruber albus*
EU012468	*Globigerinoides*	*ruber albus*
MN384216	*Globigerinoides*	*tenellus*
MN383701	*Globigerinoides*	*tenellus*
EU012479	*Globigerinoides*	*elongatus*
AB263465	*Globigerinoides*	*conglobatus*
AB263466	*Globigerinoides*	*conglobatus*
MN384152	*Globigerinoides*	*conglobatus*

RESULTS

We succeeded in extracting 260 specimens belonging to the *G. falconensis* plexus from samples ranging from Zone M5 (*sensu* Wade *et al.* 2011) to Recent from multiple global locations (Fig. 2). The specimens of the *G. falconensis* plexus could always be distinguished from *G. bulloides* by the distinctive apertural lip. During our examination we noted a difference in the overall shape of the test of the recent specimens. While Miocene populations possess a morphology consistent with the holotype designated by Blow (1959), the Pliocene and Quaternary populations, in contrast, exhibit a more lobate outline in umbilical view, with a tendency for chamber elongation and a flatter spiral side. These characters are not present in the Miocene specimens, deviating from the holotype of *G. falconensis*. *Globigerina falconensis s.s* is still present in modern assemblages, but the overall number of such individuals is lower than that of lobulate individuals.

Supporting these preliminary observations, the key parameters we measured have different values (e.g. roundness, or the lobateness of the outline) through the fossil record. In Figure 3, the distribution of two parameters (roundness and maximum diameter) shows a marked shift in the occupancy of the morphospace through time, with the Recent populations (average roundness = 1.21) being significantly different from the Miocene populations (average roundness = 1.12). This difference is not related to the size of the specimens

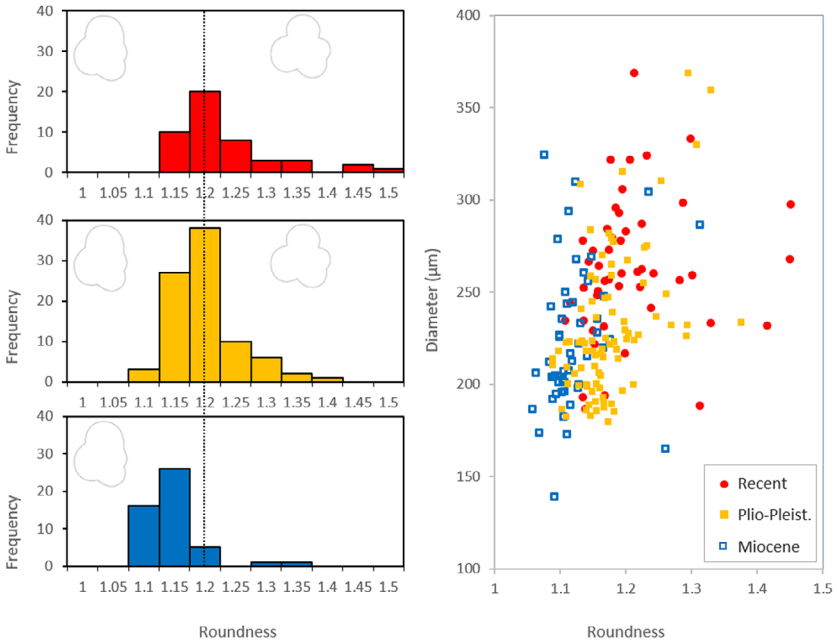

FIG. 3. On the left, histograms represent the temporal shift in the mean values of the roundness (R), highlighting the development of a progressively more lobate test in the *G. falconensis* plexus after the late Miocene. The mean value of R in the Miocene specimens is 1.12, and it reaches 1.20 during the Pliocene to Recent interval. Modern mean value (R = 1.20) is indicated by the dotted vertical line. Miocene specimens are represented in blue, Plio-Pleistocene ones in yellow and Recent specimens in red. The outlines of the two morphotypes are drawn at the top of each histogram illustrating the differences in roundness. The cross plot on the right shows the measured values of diameter (D) vs roundness (R). The specimens are represented by different symbols according to their stratigraphic age: Miocene with blue empty squares, Plio-Pleistocene with yellow squares and Recent with red circles. These plots show how R is the key parameter describing the morphological evolution through time of the *G. falconensis* plexus.

analysed (Fig. 3). The change through time is such that the Recent specimens plot outside of the range of variability recorded in the Miocene populations. Pliocene and Pleistocene populations still retain individuals comparable to *G. falconensis s.s.* but the frequency of the lobulate types is consistently higher (Fig. 3).

Wall texture

While investigating the lineage morphology, we noted unexpected differences and variability in the wall texture of the specimens. Comparison of the different Recent *G. falconensis* populations investigated globally and *G. bulloides* specimens are illustrated Figure 4. Normally the wall texture of *G. falconensis* is reported in the literature as *bulloides*-type (Fig. 4), as in its ancestor species *G. bulloides*. We measured the pore number and mean diameter in a standard area of 50 × 50 µm. Our data indicate a difference between the *G. falconensis* plexus and the other globigerinids (Fig. 5). The average measured pore diameter is 1.7 µm, but the size interval spans from 3.0 to 1.0 µm. The total number of pores in the standard unit areas ranges from 20 to 55, with 32 as the mean value. The range of the *G. falconensis* plexus overlaps the 'morphospace' typical of *Globoturborotalita*, with slightly larger pores than *G. bulloides* (Fig. 5). No substantial differences emerged between modern and fossil specimens of the *G. falconensis* plexus (Fig. 5), which showed consistent values through space and time.

Modern specimens from the Atlantic Ocean at different latitudes have been imaged for comparison with the Arabian Sea populations (Meteor M32/2). These specimens are shown in Figure 4 together with *G. bulloides* from the same assemblages, in order to document the difference in wall texture between the two taxa. The main discriminant between the two morphospecies is the development or partial development of inter pore ridges in the *G. falconensis* plexus. We refer to this wall texture as pseudocancellate. The development of interpore ridges is absent in *G. bulloides*, and it is indeed considered a key feature of other genera, such as *Globoturborotalita*, *Globigerinoides* and *Trilobatus*. Therefore, we felt compelled to re-examine the phylogenetic position of the *G. falconensis* lineage using the modern molecular genetic sequences available as an independent source of information.

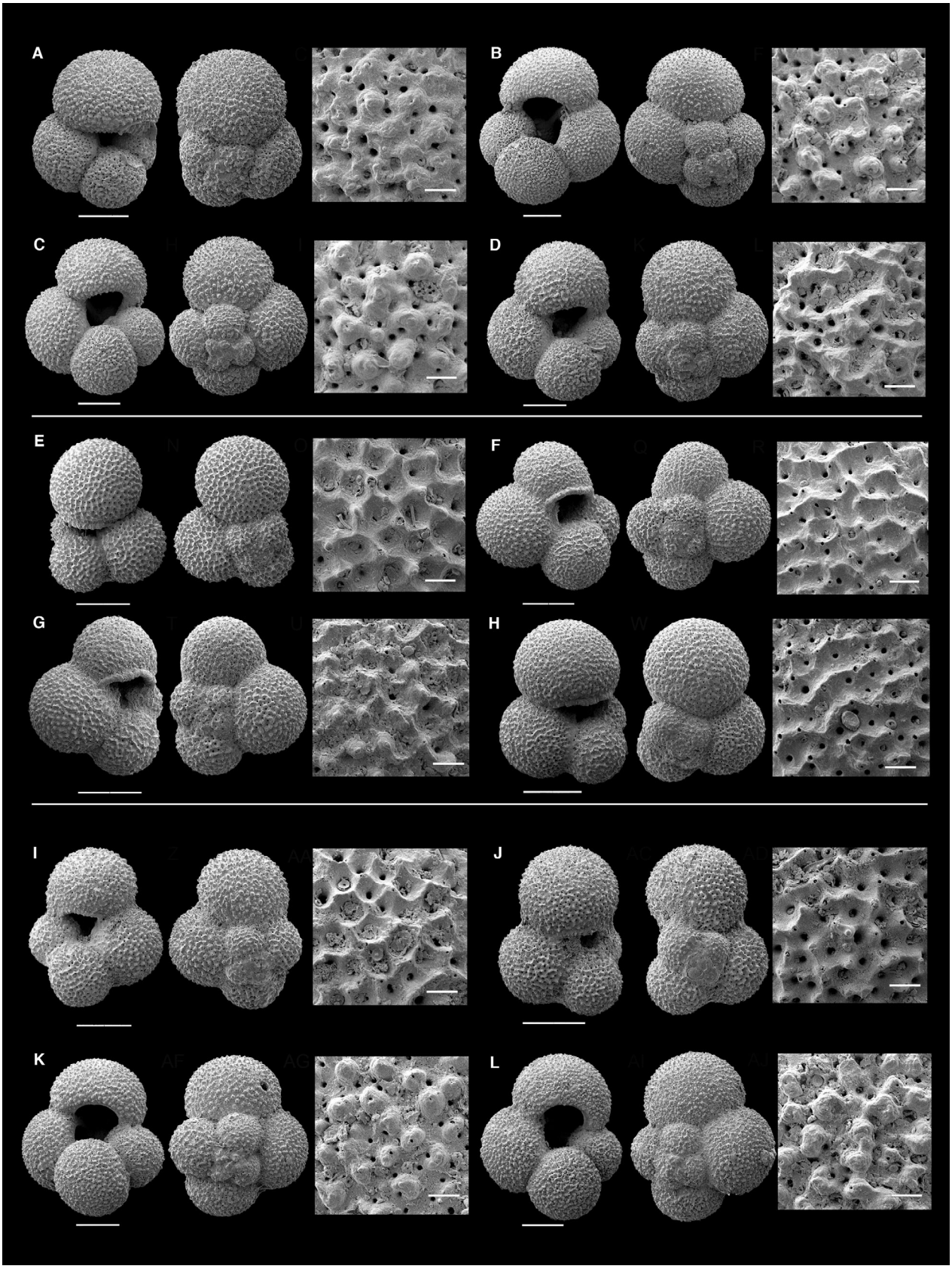

FIG. 4. Scanning electron micrographs of *Globigerina* sp. from Zone PT1, showing wall texture and range of morphological variability. A, NHMUK ZF 9968, ODP Hole 984A 1H CC, North Atlantic. B, NHMUK ZF 9971, ODP Hole 984A 1H CC, North Atlantic. C, NHMUK ZF 9972, ODP Hole 984A 1H CC, North Atlantic. D, NHMUK ZF 9973, ODP Hole 984A 1H CC, North Atlantic. E, NHMUK ZF 9965, ODP Hole 925B 1H CC, equatorial west Atlantic. F, NHMUK ZF 9967, ODP Hole 925B 1H CC, equatorial west Atlantic. G, NHMUK ZF 9966, ODP Hole 925B 1H CC, equatorial west Atlantic. H, NHMUK ZF 9964, ODP Hole 925B 1H CC, equatorial west Atlantic. I, NHMUK ZF 9969, ODP Hole 662B 1H CC, equatorial east Atlantic. J, NHMUK ZF 9970, ODP Hole 662B 1H CC, equatorial east Atlantic. K, NHMUK ZF 9974, ODP Hole 662B 1H CC, equatorial east Atlantic. L, NHMUK ZF 9975, ODP Hole 662B 1H CC, equatorial east Atlantic. Scale bars represent: 100 μm (main images); 10 μm (details of wall texture).

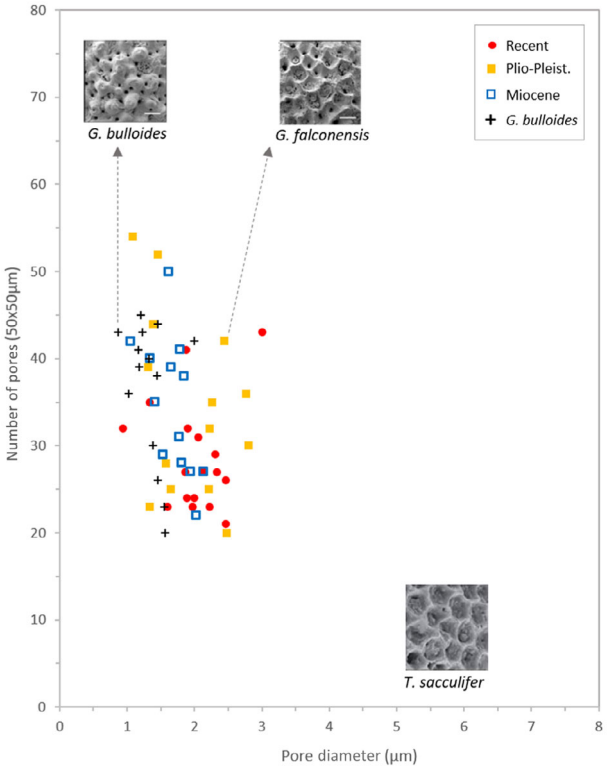

FIG. 5. Wall texture diagram showing the concentration of pores per 50 × 50 μm surface area (modified after Bé 1968). *Globigerina falconensis* plexus and has similar values to *G. bulloides*. The same colour code from the previous figures is applied here (Miocene in blue, Plio-Pleistocene in yellow and Recent in red).

Genetic results

We selected SSU rDNA sequence extracted from single cells and attributed to *G. falconensis* collected in the Great Barrier Reefs, and available in the PR^2 database (Guillou *et al.* 2013). The topology obtained shows the phyletic relation between *G. falconensis* and the other genera of Globigerinidae, such as *Globoturborotalita*, and *Globigerinoides* (Fig. 6).

The resulting tree places *G. falconensis* as a distinct clade to *Globigerinoides* and *Globoturborotalita rubescens*. The molecular clock calibrated on divergences within *Globigerinoides* and *Globoturborotalita rubescens* indicates an ancient split between the *G. falconensis* plexus and *Globoturborotalita* estimated at around 29 Ma, in the early Oligocene. This split is then much older than the complete fossil record of *G. falconensis*, which appeared around 17 Ma (early Miocene). This datum demonstrates that *G. falconensis* and *Globoturborotalita* have a significant degree of genetic divergence, indicating that they are not closely related. Additionally, this suggests that *G. falconensis* belongs to the genus *Globigerina* with its sister taxon and ancestor *G. bulloides*.

DISCUSSION

Globigerina falconensis *plexus*

We aimed to link the extant and fossil record of the *G. falconensis* plexus and use morphometric data to determine the variability of the plexus and link the holotype of *G. falconensis*, (early Miocene) with the modern populations. Both visually and quantified by our morphometric analysis, there is a difference in the shape of the test in the Recent specimens, which exhibit a more lobate outline, with a tendency for chamber elongation and a lower trochospire. Our morphometric and genetic data thus present a conundrum. There are two morphotypes in the modern ocean, both possessing four chambers in the final whorl, and a lip, but they are distinguished by the periphery. The lobulate morphospecies is inconsistent with the holotype of *G. falconensis*, which is much more compact (Fig. 7). The more lobate morphology is not found in the fossil record in sediments before the upper Miocene, while the compact *G. falconensis s.s.* persists up to the modern. There are specimens that can be attributed to *G. falconensis s.s.* in Recent sediments, but these are smaller in size and rare. Our morphometric and imaging study suggests that there

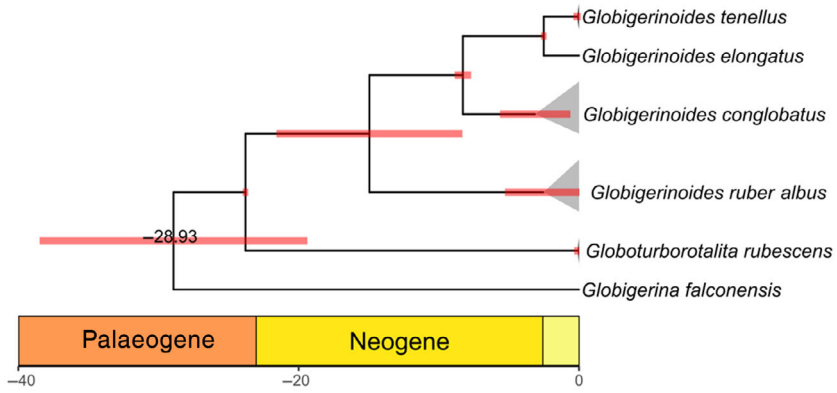

FIG. 6. Molecular clock estimates of the diversification of the *Globigerina falconensis* plexus from the genera *Globoturborotalita* and *Globigerinoides*. The genera separated in the early Oligocene (28.93 Ma), before the appearance of *G. falconensis* in the fossil record, neglecting any direct phylogenetic link between the two lineages. The pink bars indicate the uncertainties in the dating each node; grey shading at tips represents the intraspecific variability.

are two types of *G. falconensis* extant in the modern ocean, one with a lobate periphery which evolved in the late Miocene, and *G. falconensis s.s.* which evolved in the early Miocene. The holotype of *G. falconensis* is representative of the variability observed in the Miocene, thus we suggest that a new species and concept is needed for the late Miocene to Recent representatives of the lineage. Therefore, to bridge the extant and fossil record and resolve the current inconsistency between the *G. falconensis* holotype and the modern morphotype, we describe the new morphospecies *G. neofalconensis*. Using mean values from the biometric parameters among the best-preserved modern specimens, we selected the type specimens (Figs 7, 8) for the new taxon (see Systematic Palaeontology, below).

Our observations indicate that the modern lobate and flatter morphology emerged in Zone M13 (late Miocene) (Fig. 9). The values extrapolated also allowed a global comparison, showing how in all sites, the lobate forms of the *falconensis* plexus were the most abundant in Recent sediments and consistently different from *G. bulloides*. In all the Recent sediments studied, a minority of *G. falconensis* specimens with a compact test and pseudocancellate wall texture were present in the smaller size fraction (<150 μm), indicating that *G. falconensis s.s.* remains extant but rare. Most specimens from sediments younger than Pliocene age are lobate, and consistent with *G. neofalconensis*.

Bringing together genetic and imaging analyses

The conundrum concerning the lobate morphology is then solved with the identification in the fossil record of *G. neofalconensis* after the late Miocene. The wall texture inconsistency still requires some further discussion. *Globigerina falconensis* has always been considered to be related to *G. bulloides* (Blow 1959, 1969; Kennett & Srinivasan 1983; Bolli *et al.* 1985; among others) and part of the genus *Globigerina*, sharing the same type of wall texture. Specimens of *G. bulloides* showing their characteristic wall texture of small and irregularly distributed pores, lacking prominent inter-pore ridges are illustrated in Figure 4. Our analysis and measurements on wall texture from specimens of the *G. falconensis* plexus ranging from the early Miocene to the Recent, indicate a high degree of variability (Fig. 4). In several instances in both fossil and modern populations, we find specimens with a pseudocancellate appearance in the earlier chambers, developing into more of a *bulloides*-type wall texture in the final and penultimate chambers. The SEM and micro-CT images (Figs 4, 7) reveal that this pseudocancellate appearance is not honeycomb-like as in the *sacculifer*-type wall texture, typified in the modern *Trilobatus sacculifer* and many fossil species (Hemleben & Olsson 2006), but the pseudocancellate texture results from larger pores and interconnecting ridges (Figs 4, 7).

The molecular clock calibrated age of the split between *G. falconensis* and *Globigerinoides–Globoturborotalita*

FIG. 7. Scanning electron and optical micrographs of holotype specimens: A–F, *Globigerina neofalconensis* sp. nov. NHMUK ZF 9958 (holotype), M32/2MC6, Arabian Sea, Holocene (Zone PT1): A–C, micro-CT images; D–F, optical micrographs. G–L, *G. falconensis* Blow, 1959, USNM MO 625697 (holotype; Smithsonian Institution), Falcón (Venezuela), early Miocene (Zone M5): G–I, SEM micrographs; J–L, optical micrographs. Scale bars represent 100 μm.

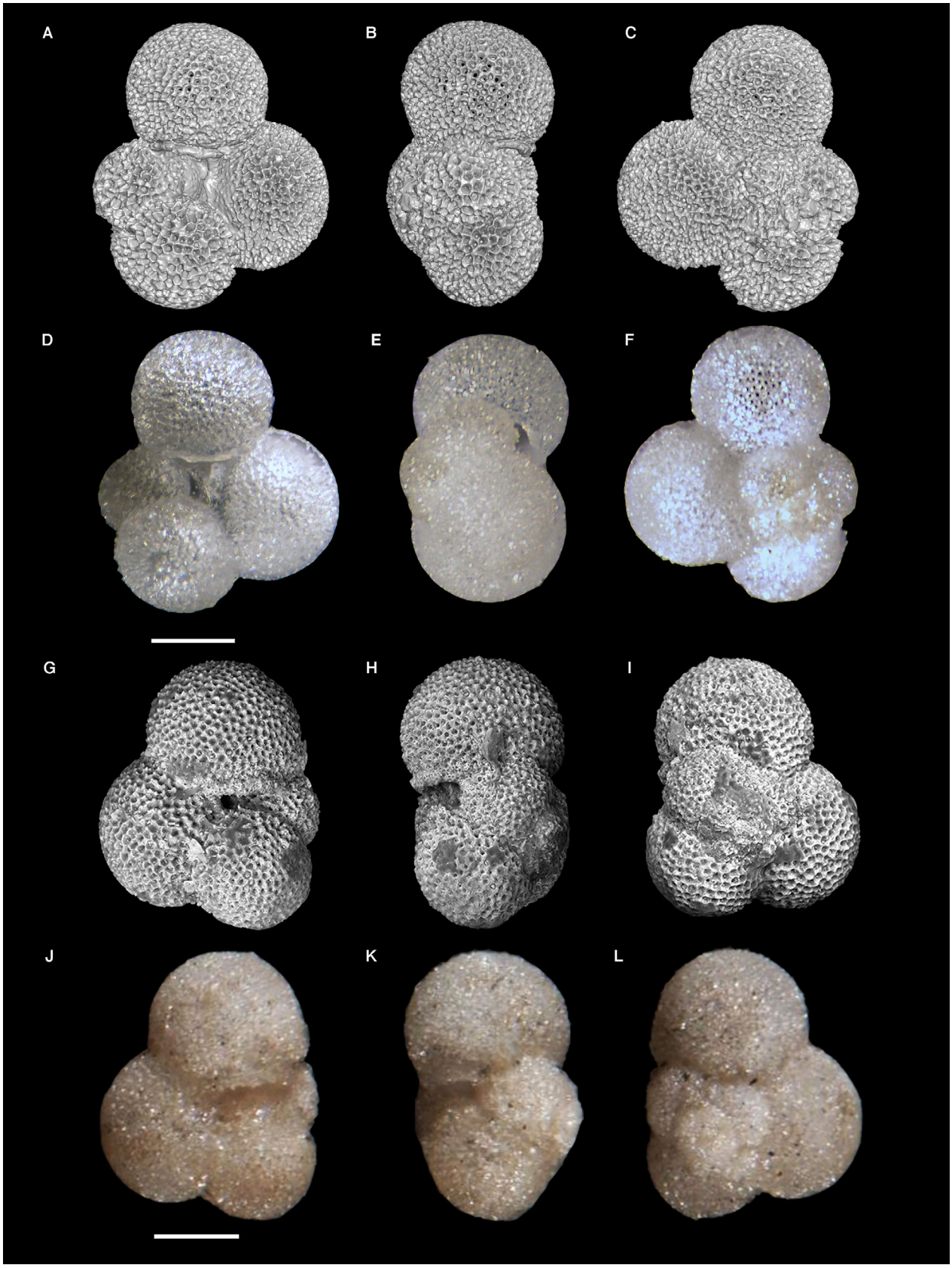

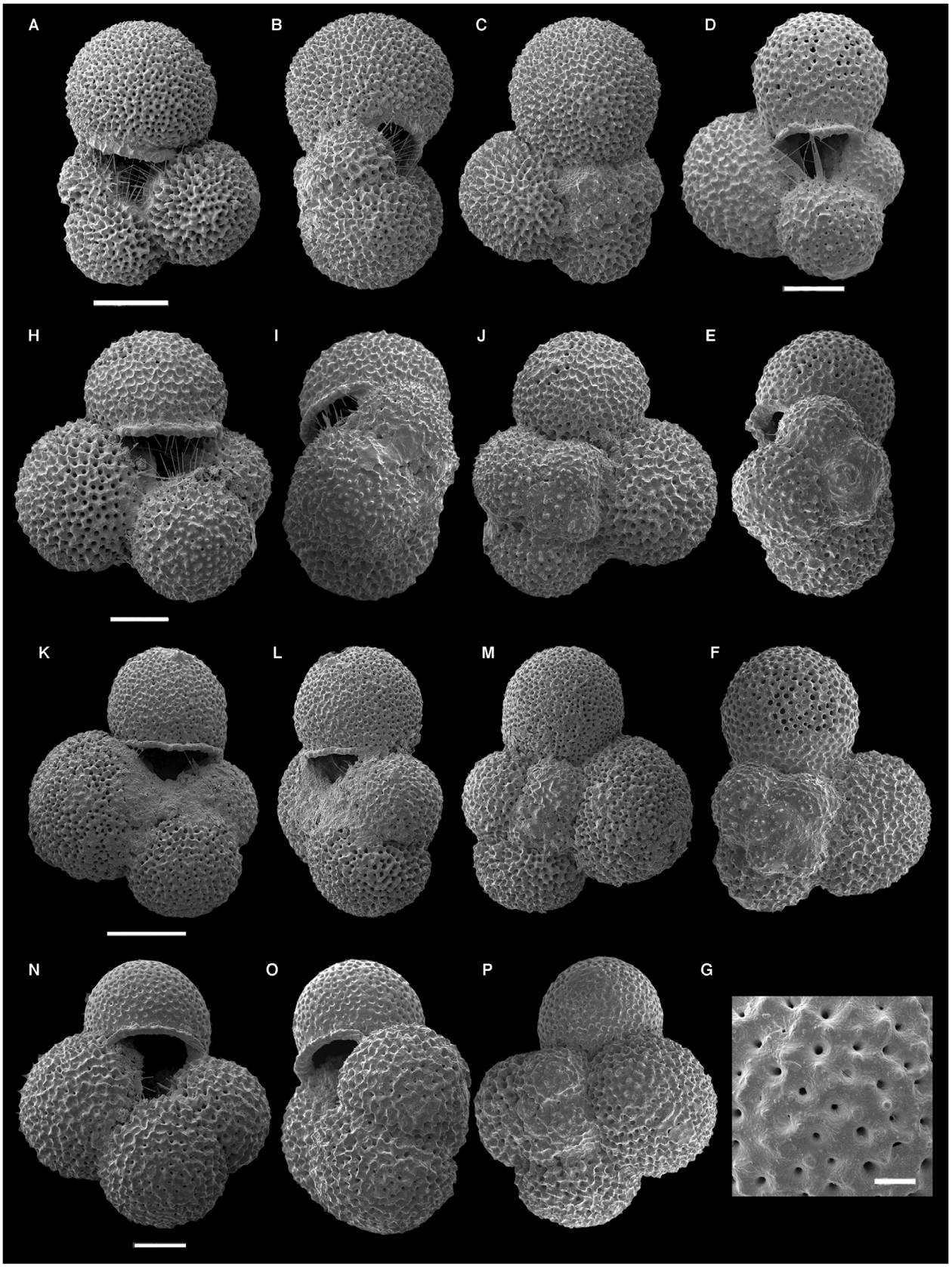

FIG. 8. *Globigerina neofalconensis* sp. nov. paratypes. A–C, NHMUK ZF 9959, M32/2MC3 0–2 cm, size fraction 200–250 μm, Arabian Sea (Zone PT1). D–G, NHMUK ZF 9961, M32/2MC3 0–2 cm, size fraction 150–200 μm; G, 50 × 50 μm wall texture detail showing *bulloides*-type wall on the 3rd ultimate chamber. H–J, NHMUK ZF 9963, M32/2MC6 0–2 cm, size fraction 150–200 μm. K–M, NHMUK ZF 9960, M32/2MC3 0–2 cm, size fraction >400 μm. N–P, NHMUK ZF 9962, M32/2MC6 0–2 cm, size fraction 200–150 μm. Scale bars represent: 100 μm (A–C, H–P); 50 μm (D–F); 10 μm (G).

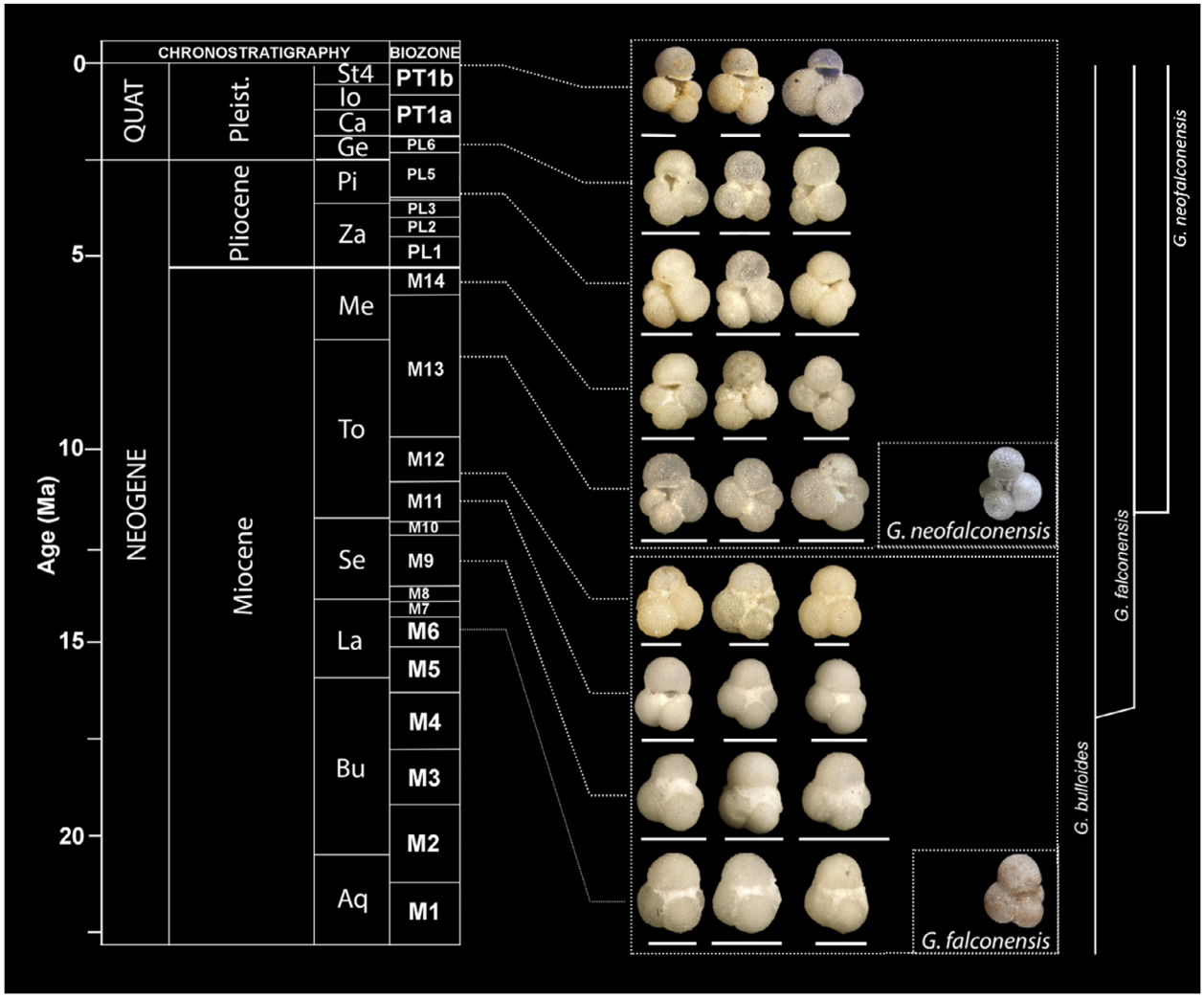

FIG. 9. Synthesis of the morphological evolution of *Globigerina falconensis* plexus. Each group of specimens is correlated to its corresponding zone (Wade *et al.* 2011). The phylogenetic relationship between the *G. falconensis* group and *G. bulloides* is shown on the right. The holotypes of *G. falconensis* and *G. neofalconensis* sp. nov. are illustrated inside the boxes on the side as a reference. All presented specimens are among the individuals measured for the biometric study herein (Zone M6–M11 specimens from ODP Site 590; Zone M12–PT1 from IODP Site U1482; Recent specimens from M32/2MC6). All scale bars represent 200 μm.

(Fig. 6) shows the ancient separation of these groups and thus confirms the higher genetic similarity of *G. falconensis* with *G. bulloides* (Stewart *et al.* 2001). These observations indicate the *G. falconensis* lineage must be retained in the genus *Globigerina* despite the difference in wall texture.

The genus *Globigerina* d'Orbigny, 1826, has been amended several times considering different criteria, from the morphology to wall texture (Bolli 1957; Blow 1959; Kennett & Srinivasan 1983; Bolli *et al.* 1985; Spezzaferri 1994; Pearson *et al.* 2006; Spezzaferri *et al.* 2018; among others). The milestone works of Bé (1968) and

Fleisher (1974) changed the taxonomy of planktonic foraminifera radically, making characters of the test wall (pore size and wall features) significant for the first time.

Following the taxonomical guidelines applied in the recent literature, wall texture is the key feature used to classify planktonic foraminifera (Bé 1968; Kennett & Srinivasan 1983; Bolli *et al.* 1985; Olsson *et al.* 1999; Pearson *et al.* 2006; Aze *et al.* 2011; Wade *et al.* 2018). The holotypes of both *G. falconensis* and *G. neofalconensis* (Fig. 7) present the same pseudocancellate wall texture not consistent with the current definition of the genus *Globigerina* (Bé 1968; Kennett & Srinivasan 1983; Bolli *et al.* 1985; Olsson *et al.* 1999; Pearson *et al.* 2006; Wade *et al.* 2018). Either the pseudocancellate wall texture evolved independently twice in the lineage, complicating the definition of *Globigerina* or this character remerged from the genetic past of the genus. In this context, the apparently pseudocancellate wall in *G. falconensis* lineage (Fig. 4) must fall within the range of variability of the *Globigerina*-type wall. Further studies are necessary to understand how this wall type can develop. A possible answer might arise from the genetic history of the genus *Globigerina*.

The earliest Globigerinidae also had a cancellate wall (*Eoglobigerina* in the Danian, early Paleocene). Such wall texture diversified during the radiation of the clade until the *bulloides*-type wall emerged in the Eocene from the cancellate genus *Subbotina*. Although *Globigerina officinalis* is the first member of its genus in the middle Eocene, the first occurrence of the true *bulloides*-type wall predates this species in its ancestor *Subbotina crociapertura* or *Subbotina roesnaesensis*. These taxa were retained by Olsson *et al.* (2006) in *Subbotina* despite already having the *Globigerina*-type wall texture. Moreover, when the genus *Globigerina* emerged, the wall texture was still variable as shown by individuals of *G. officinalis* presenting different types of wall texture on different portions of their test (Olsson *et al.* 2006; Spezzaferri *et al.* 2018). Eventually with the appearance of *G. archaeobulloides* and *G. bulloides* the wall texture became consistently *bulloides*-type. Since the *G. falconensis* lineage belongs to the same clade as *G. bulloides*, the pseudocancellate wall texture must have re-emerged in the Miocene. The phenotypic plasticity of planktonic foraminifera might allow similar wall textures to emerge repeatedly through time (Kendall *et al.* 2020). Alternatively, if the emergent character is similar to the plesiomorphic state, all descendants could retain it. Thus, all Globigerinidae might have retained the ability to build a pseudocancellate wall, suppressed in certain species like *G. bulloides*, and expressed in others as in the *G. falconensis* lineage. The specimens with a mixed wall texture could indeed demonstrate plasticity during ontogenetic development expressing traits from the genetic past of the lineage. These arguments would benefit from focused research on both modern and fossil planktonic foraminifera.

Molecular data indicate that there is only one form of *G. falconensis* in the modern ocean that is closely related to *G. bulloides* (e.g. Brummer & Kučera 2022). Thus, the description of a new morphospecies, *G. neofalconensis*, aligns with the morphological but not with the genetic evidence. A similar situation is not new in planktonic foraminifera and it finds its best example in *T. sacculifer* plexus, which consists of four extant morphospecies *T. sacculifer* (Brady 1877), *T. quadrilobatus* (d'Orbigny 1846), *T. immaturus* (LeRoy 1939) and *T. trilobus* (Reuss 1850). Each of these morphospecies has a different biogeography and stratigraphic history (Poole 2017), but molecular genetic and culturing studies of extant specimens (e.g. Hemleben *et al.* 1987; André *et al.* 2014) suggests that all four morphospecies belong to the same biological species. The variation between the morphospecies within the *T. sacculifer* plexus is considered to be ecophenotypically controlled (e.g. Hecht & Savin 1972; Hecht 1974; André *et al.* 2014; Schmidt *et al.* 2016). Morphological studies on fossil specimens (Poole & Wade 2019) support the hypothesis that *T. sacculifer* plexus morphospecies are the same biological species, but highlight the necessity to retain the morphospecies in order to increase their biostratigraphical and palaeoecological value. We applied here the same principle to the *G. falconensis* plexus, to retain as much information as possible through its stratigraphic record and evolution.

SYSTEMATIC PALAEONTOLOGY

Institutional abbreviation. NHMUK, Natural History Museum, London, UK.

Order FORAMINIFERIDA d'Orbigny, 1826
Superfamily GLOBIGERINOIDEA Carpenter, Parker & Jones *in* Carpenter, 1862
Family GLOBIGERINIDAE Carpenter, Parker & Jones *in* Carpenter, 1862
Genus GLOBIGERINA d'Orbigny, 1826

Type species. Globigerina bulloides.

Diagnosis. Normal perforate, spinose *bulloides*-type and pseudocancellate wall structure. Aperture umbilical with no supplementary apertures present.

Test morphology. Low trochospiral, lobulate outline, chambers globular; 3–5 slightly embracing chambers in ultimate whorl, increasing slowly in size, sutures straight and moderately depressed; umbilicus large, open, enclosed by surrounding chambers; aperture umbilical, a broad arch, which may be bordered by an imperforate thin rim or lip.

Remarks. The first representative of the genus is *G. officinalis*, emerging in middle Eocene Zone E10 (Olsson *et al.* 2006). The genus diversified in the Oligocene (Wade *et al.* 2018).

Range. Eocene–present.

Globigerina falconensis Blow, 1959
Figure 7G–L

	1959	*Globigerina falconensis* Blow, pl. 9, fig. 40.
	1969	*Globigerina falconensis* forma typica-metatype; Blow, pl. 16, fig. 1.
	1979	*Globigerina falconensis*; Poore, figs 10–12.
	2012	*Globigerina falconensis*; Beldean *et al.*, pl. 3.1, figs 2–3.
non	1960	*Globigerina bollii* Cita & Premoli Silva, fig. 1a–c.
non	1972	*Globigerina antarctica* Keany & Kennett, fig. 6.
?	1969	*Globigerina nilotica* Viotti & Mansour, fig. 1a–c.

Test morphology. Wall spinose, normal perforate, mean pore size 1.7 μm, mean pore concentration 32 per unit area (2500 μm^2). The wall texture is variable ranging from a *bulloides*-type pitted surface to a pseudocancellate texture, with coalescing ridges arranged around the pores, creating a honeycomb appearance (Figs 4, 7). Test low trochospiral with ten to twelve chambers arranged in about two whorls and with four subspherical chambers in the last whorl. Random coiling, but with a tendency for predominately sinistral. Subspherical chambers, slightly embracing, especially the last chamber, increasing regularly and slowly in size as added, and separated by slightly incised straight sutures. The umbilicus is small and deep, sometimes almost closed by the strongly developed lip on the last chamber. The umbilical aperture is an elongate low arch, sometimes slit-like, almost straight, with a well-developed imperforate lip. Umbilical sutures are straight and radial, but not strongly incised. In spiral view, all chambers of the trochospire are visible, subspherical and separated by radial and straight to slightly curved sutures, weakly incised.

Size. Maximum diameter of the holotype: 320 μm.

Remarks. Distinguished from *G. neofalconensis* by a closer umbilicus, a more compact test due to the tighter coiling, and with less incised sutures. *Globigerina falconensis* can be distinguished from *G. bulloides* by a well-developed apertural lip, narrower, lower-arched aperture, and the presence of a cancellate honeycomb wall texture. The coiling direction is reported in the literature as random (Blow 1959, 1969), but based on our observation the two subspecies tend to have a different preferential coiling direction. Within our dataset, *G. falconensis* is predominantly left coiling, while *G. neofalconensis* has a random coiling.

Globigerina falconensis shows commonalities with some taxa belonging to the genus *Globoturborotalita* bearing four chambers in the final whorl and an apertural lip or rim, such as *Gt. ouachitaensis*, *Gt. druryi*, *Gt. occlusa* and *Gt. eolabiacrassata*. *Globigerina falconensis* can be differentiated from *Gt. ouachitaensis* due to its thicker and more developed apertural lip, the lower-arched aperture and the overall compact morphology and commonly larger size. *Globoturborotalita druryi* is characterized by a thicker apertural lip, larger size than *G. falconensis*, a more compact test outline and a higher trochospire visible when observed in edge view. *Globigerina falconensis* is distinguished from *Globoturborotalita occlusa* by the consistently developed apertural lip, which is sometimes absent in *Gt. occlusa*, and by its more compact shape, while *Gt. occlusa* tends to be lobulate and present more incised sutures with spherical chambers. *Globoturborotalita eolabiacrassata* can be separated from *G. falconensis* by tighter coiling, smaller size, more coarsely perforated test and a shorter-arched umbilical aperture, bordered by a thick imperforated rim.

Range. Burdigalian (Zone M5) – present.

Globigerina neofalconensis sp. nov.
Figures 7A–F, 8

	1962	*Globigerina falconensis*; Parker, pl. 1, fig. 17–19.
	1969	*Globigerina falconensis* forma atypica; Blow, p. 319.
	1971	*Globigerina falconensis*; Brönniman & Resig, pl. 3, figs 6–7.
	1971	*Globigerina* aff. *G. falconensis*; Brönniman & Reisig, fig. 9.
	1971	*Globigerina falconensis*?; Brönniman & Resig, pl. 3, fig. 8.
	1977	*Globigerina falconensis*; Malmgren & Kennett, pl. 1, figs 3, 5, 6.
	1979	*Globigerina falconensis*; Iaccarino & Salvatorini, pl. 1, fig. 14.
	1979	*Globigerina falconensis*; Thunnell *et al.* pl. 1, fig. 8.
	1986	*Globigerina falconensis*; Jenkins *et al.* pl. 1, figs 5–6.
	2007	*Globigerina falconensis*; Dowsett & Robinson pl. 1, fig. 7.
	2008	*Globigerina falconensis*; Parcerisa *et al.*, fig. 5d.
	2010	*Globigerina falconensis*; Ovechkina *et al.*, fig. 6A–C.
	2017	*Globigerina falconensis*; Schiebel & Hemleben, pl. 2.4, figs 1–11.
	2020	*Globigerina falconensis*; Lam & Leckie, pl. 3, figs 17–18.
?	1971	*Globorotalia* (*Turborotalia*) *palpebra* Brönniman & Resig, pl. 3, fig. 3.

LSID. https://zoobank.org/NomenclaturalActs/959F1817-6657-43C1-8B25-5581CC37C0FA

Derivation of name. Named after its ancestor *G. falconensis* with the Greek prefix 'neo' meaning 'new'.

Type specimens. Holotype NHMUK ZF 9958; paratypes NHMUK ZF 9959, NHMUK ZF 9960, NHMUK ZF 9961, NHMUK ZF 9962, NHMUK ZF 9963. The holotype specimen has been CT-scanned (https://doi.org/10.17602/M2/M567220).

Diagnosis. Type of wall: Spinose, pseudocancellate and *bulloides*-type wall texture. The final chamber tends to be smoother with

visibly variable pore size. The penultimate chamber is commonly pseudocancellate, the third ultimate can instead present a *Globigerina*-type wall. Sometimes specimens with completely pseudocancellate wall occur, showing that the ontogenetic pattern is inconstant.

Test morphology: Test loosely coiled constituted by four subspherical slowly increasing chambers in the final whorl. The outline is lobate. A total of 10–12 chambers are arranged in 2–2.5 whorls, with random coiling direction. In umbilical view, the last whorl consists of subspherical chambers loosely coiled and separated by straight and incised sutures. The shape of the last chamber is quite variable, sometimes developing an elongated bulb-like shape, though kummerforms are very common. Umbilicus deep and open, a low umbilical aperture bordered with an evident imperforate lip. The aperture can create a curved shape of the lip. In spiral view, four subspherical chambers divided by straight incised sutures, all the chambers from the previous whorls are visible in the spire. In edge view, low trochospire and flat spiral side with the last chamber sometimes slightly tilted towards the umbilicus, margin rounded.

Size. The maximum diameter of the holotype is 340 μm.

Remarks. This new species is named after its ancestor *G. falconensis*, to retain a well-established and widely used taxonomical name and concept. *Globigerina neofalconensis* can be distinguished from its ancestor *G. falconensis* by its more lobate profile and a more loosely coiled test, coupled with a wider umbilicus (see Table 2; Figs 7, 8). Blow (1969) reported two different types of *G. falconensis* showing distinct stratigraphic ranges, named *G. falconensis* forma typica and *G. falconensis* forma atypica. The new species presented here matches with the latter, in terms of the overall morphology and stratigraphic range.

TABLE 2. Key taxonomical features to distinguish *G. neofalconensis* from its ancestor *G. falconensis*.

	G. falconensis	*G. neofalconensis*
Coiling	Low trochospiral	Low trochospiral
Number of whorls	2	2–2.5
Chambers in final whorl	4	4
Last chamber	Subspherical slightly embracing	Subspherical to elongated
Profile	Compact	Lobate
Margin	Rounded	Rounded, flat spiral side
Sutures	Radial, depressed	Radial and deeply incised
Primary aperture	Low arched symmetrical, umbilical with a lip	Low straight symmetrical, umbilical with a lip
Umbilicus	Narrow and deep	Open to wide and deep
Wall texture	Spinose, pseudocancellate	Spinose, pseudocancellate and *bulloides*-type

Globigerina neofalconensis can possess both a pseudocancellate and *bulloides*-type wall texture. The variability in the wall texture in the different chambers as added is not always evident, making its recognition complex. Specimens of *G. neofalconensis* with a fully developed *bulloides*-type wall texture have been reported by various authors (Brönnimann & Resig 1971; Srinivasan 1975; Bé *et al.* 1977; Malmgren & Kennett 1977; Thunnell 1979; Jenkins *et al.* 1986; Hemleben *et al.* 1989; Iaccarino & Salvatorini 1979; Dowsett & Robinson 2007; Parcerisa *et al.* 2008; Lam & Leckie 2020; Schiebel & Hemleben 2017). Culture studies have indicated that pore size can be plastic and influenced by temperature and metabolic rate (Burke *et al.* 2018) and thus some of the variability in wall texture appearance may be due to environmental influences.

Globigerina neofalconensis is distinguished from *G. bulloides* by its apertural lip, the low aperture and the very lobate profile. Commonly the last chamber of *G. neofalconsis* can be kummerform or radially elongated and bulb shaped. Both of these features are absent or rare in *G. bulloides*. *Globigerina neofalconensis* can be differentiated from *G. antarctica* due to its coarser and hispid wall texture, the well-developed apertural lip and in having four chambers in the last whorl, while sporadically individuals of *G. antarctica* may have five chambers in the final whorl, they are always characterized by a thin wall texture and a very thin lip.

Globigerina neofalconensis can be compared with various species within *Globoturborotalita*, such as, *Gt. foliata*, *Gt. ouachitaensis*, *Gt. pseudopraebulloides* and *Gt. occlusa*. *Globigerina neofalconensis* can be distinguished from *Gt. foliata* because of its apertural lip and wider umbilicus. *Globigerina neofalconensis* differs from *Gt. ouachitaensis* by its bigger size, more open umbilicus and interomarginal aperture bordered by a thicker lip. *Globigerina neofalconensis* can be also distinguished from *Gt. pseudopraebulloides* thanks to the apertural lip, and the lower aperture and flatter spiral side. *Globigerina neofalconensis* differs from *Gt. occlusa* in having a longer aperture bordered by a lip and having a looser coiling.

In the literature, there are several examples of attempted reclassification of *G. falconensis*. Brönnimann & Resig (1971) described different globigerinids belonging to the *G. falconensis* group. They reported the presence of different morphotypes under the name *G. falconensis* and suggested the possibility of a group of taxa that are quasi-homeomorphic to *G. falconensis*. Anomalies were noticed in the wall texture and used as a possible base to untangle the controversy (Brönnimann & Resig 1971). We consider all the specimens to be *G. neofalconensis*, despite the different wall texture in the individuals shown in this paper. However, we retain in *G. falconensis* all the specimens described by Brönnimann & Resig (1971) with a tighter coiling, more compact and thicker test. We also consider *Globorotalia palpebra* (Brönnimann & Resig 1971) to be taxon inquirendum, due to the lack of information, and its absence from other studies published in literature, and its overall rarity.

Range. Tortonian (Zone M13) – present.

CONCLUSION

We have endeavoured to link the extant and fossil records of *Globigerina*, focusing on the species *G. falconensis* described from early Miocene sediments, and still alive in the oceans today. We investigated specimens of the *G. falconensis* plexus from the modern and fossil record with an integrated approach. Our morphometric and microscopy studies reveal that the majority of extant forms commonly found in the modern oceans are more lobate, and loosely coiled, and not consistent with the fossil holotype of *G. falconensis*. We therefore name a new morphospecies *G. neofalconensis* to resolve the conflict between the type specimen of *G. falconensis* and the living populations. The new morphospecies *G. neofalconensis*, evolved in the late Miocene and inhabits the present oceans coexisting with rarer populations of *G. falconensis s.s.* Scanning electron microscopy highlighted how this entire plexus presents a peculiar wall texture, different to the typical *bulloides*-type, which characterizes the genus *Globigerina*. This apparent inconsistency of the wall texture led us to approach the lineage from a genetic perspective. Our molecular analysis indicates that *G. falconensis* and *Globorturborotalita* lineages split at an estimated 29 Ma, in the Oligocene. This age predates the existence of *G. falconensis* in the fossil record, and thus excludes any direct phylogenetic link between this species and the *Globoturborotalita* plexus, supporting the hypothesis that the two are clearly separated lineages. All these data allowed us to retain the new morphospecies *G. neofalconensis* within the genus *Globigerina*.

Acknowledgements. This research was supported by Natural Environment Research Council grant NE/P019013/1 to BW and NE/P019269/1 to THGE. MK acknowledges funding by the Cluster of Excellence 'The Ocean Floor—Earth's Uncharted Interface' (EXC 2077, grant no. 390741603) granted through the German Research Foundation (DFG). The authors are grateful to Jim Davy for technical support in the SEM Lab at UCL. We also thank Steve Stukins from the NHM for providing access to the museum collections and Hartmut Schulz from the University of Tübingen for providing surface sediment samples from the Arabian Sea. The authors thank Paul Pearson for helpful and insightful discussions on foraminifera evolution and taxonomy and Luca Foresi for providing further samples and discussion. The authors are also grateful to Brian Huber at the Smithsonian Institution for providing holotype images of *G. falconensis*. The authors are also grateful to Geert-Jan Brummer, Kate Darling and Raphaël Morard for the insightful discussions and comments on this work. Hartmut Schulz, Tracy Aze and a third, anonymous, referee commented on earlier versions of the manuscript.

Author contributions. **Conceptualization** A Fabbrini (AF), BS Wade (BSW); **Data Curation** AF, M Greco (MG), F Iacoviello (FI); **Formal Analysis** AF (micropalaeontology); MG (genetic data), FI (micro-CT), BSW; **Funding Acquisition** BSW, THG Ezard (THGE); **Investigation** AF; **Resources** M Kucera (MK), BSW; **Supervision** BSW; **Visualization** AF, MG, BSW; **Writing – Original Draft Preparation** AF, MG; **Writing – Review & Editing** AF, MG, FI, MK, THGE, BSW.

DATA ARCHIVING STATEMENT

This published work and the nomenclatural acts it contains have been registered with ZooBank: https://zoobank.org/References/202AA4F6-8FDE-4630-87B1-A6319802F10E. The 3D model and raw data of the holotype is available from MorphoSource: https://doi.org/10.17602/M2/M567220 (model); https://doi.org/10.17602/M2/M522833 (raw data). Biometry data are available in the Dryad Digital Repository: https://doi.org/10.5061/dryad.fbg79cp0r.

Editor. Helen Coxall

REFERENCES

AL-SABOUNI, N., FENTON, I. S., TELFORD, R. J. and KUČERA, M. 2018. Reproducibility of species recognition in modern planktonic foraminifera and its implications for analyses of community structure. *Journal of Micropalaeontology*, **37** (2), 519–534.

ANDRÉ, A., QUILLÉVÉRÉ, F., MORARD, R., UJIIÉ, Y., ESCARGUEL, G., de VARGAS, C., de GARIDEL-THORON, T. and DOUADY, C. J. 2014. SSU rDNA divergence in planktonic foraminifera: molecular taxonomy and biogeographic implications. *PLoS One*, **9** (8), e104641.

AURAHS, R., TREIS, Y., DARLING, K. and KUCERA, M. 2011. A revised taxonomic and phylogenetic concept for the planktonic foraminifer species *Globigerinoides ruber* based on molecular and morphometric evidence. *Marine Micropaleontology*, **79** (1–2), 1–14.

AZE, T., EZARD, T. H., PURVIS, A., COXALL, H. K., STEWART, D. R., WADE, B. S. and PEARSON, P. N. 2011. A phylogeny of Cenozoic macroperforate planktonic foraminifera from fossil data. *Biological Reviews*, **86** (4), 900–927.

BÉ, A. W. 1968. Shell porosity of Recent planktonic foraminifera as a climatic index. *Science*, **161** (3844), 881–884.

BÉ, A. W., HEMLEBEN, C., ANDERSON, O. R., SPINDLER, M., HACUNDA, J. and TUNTIVATE-CHOY, S. 1977. Laboratory and field observations of living planktonic foraminifera. *Micropaleontology*, **23** (2), 155–179.

BELDEAN, C., FILIPESCU, S. and BALC, R. 2012. Paleoenvironmental and biostratigraphic data for the Early Miocene of the north-western Transylvanian Basin based on planktonic foraminifera. *Carpathian Journal of Earth & Environmental Sciences*, **7** (1), 171–184.

BLOW, W. H. 1959. Age, correlation and biostratigraphy of the upper Tocuyo (San Lorenzo) and Pozón Formations, eastern Falcon, Venezuela. *Bulletins of American Paleontology*, **39**, 67–251.

BLOW, W. H. 1969. Late Middle Eocene to Recent planktonic foraminiferal biostratigraphy. 199–242. *In Proceedings of the First International Conference on Planktonic Microfossils, Geneva 1967*. Vol. **1**. EJ Brill.

BOLLI, H. M. 1957. Planktonic foraminifera from the Oligocene-Miocene Cipero and Lengua formations of Trinidad, B.W.I. *United States National Museum Bulletin*, **215**, 97–123.

BOLLI, H. M., SAUNDERS, J. B. and PERCH-NIELSEN, K. (eds). 1985. *Plankton Stratigraphy*. Cambridge University Press.

BRADY, H. B. 1877. II. Supplementary note on the Foraminifera of the Chalk (?) of the New Britain Group. *Geological Magazine*, **4** (12), 534–536.

BRÖNNIMANN, P. and RESIG, J. 1971. A Neogene globigerinacean biochronologic time-scale of the southwestern Pacific. *Initial Reports of the Deep Sea Drilling Project*, **7** (2), 1235–1469.

BRUMMER, G. J. A. and KUČERA, M. 2022. Taxonomic review of living planktonic foraminifera. *Journal of Micropalaeontology*, **41** (1), 29–74.

BURKE, J. E., RENEMA, W., HENEHAN, M. J., ELDER, L. E., DAVIS, C. V., MAAS, A. E., FOSTER, G. L., SCHIEBEL, R. and HULL, P. M. 2018. Factors influencing test porosity in planktonic foraminifera. *Biogeosciences*, **15** (21), 6607–6619.

CARPENTER, W. B. 1862. *Introduction to the study of the foraminifera*. R. Hardwicke for the Ray Society.

CITA, M. B. and PREMOLI SILVA, I. 1960. *Globigerina bollii*, nuova specie delle Langhe. *Rivista Italiana di Paleontologia*, **44** (1), 119–126.

COLETTI, G., STAINBANK, S., FABBRINI, A., SPEZZAFERRI, S., FOUBERT, A., KROON, D. and BETZLER, C. 2018. Biostratigraphy of large benthic foraminifera from Hole U1468A (Maldives): a CT-scan taxonomic approach. *Swiss Journal of Geosciences*, **111**, 523–536.

DOWSETT, H. J. and ROBINSON, M. M. 2007. Mid-Pliocene planktonic foraminifer assemblage of the North Atlantic Ocean. *Micropaleontology*, **53** (1–2), 105–126.

FABBRINI, A., ZAMINGA, I., EZARD, T. H. and WADE, B. S. 2021. Systematic taxonomy of middle Miocene *Sphaeroidinellopsis* (planktonic foraminifera). *Journal of Systematic Palaeontology*, **19** (13), 953–968.

FENTON, I. S., BARANOWSKI, U., BOSCOLO-GALAZZO, F., CHEALES, H., FOX, L., KING, D. J., LARKIN, C., LATAS, M., LIEBRAND, D., MILLER, C. G., NILSSON-KERR, K., PIGA, E., PUGH, H., REMMELZWAAL, S., ROSEBY, Z. A., SMITH, Y. M., STUKINS, S., TAYLOR, B., WOODHOUSE, A., WORNE, S., PEARSON, P. N., POOLE, C. R., WADE, B. S. and PURVIS, A. 2018. Factors affecting consistency and accuracy in identifying modern macroperforate planktonic foraminifera. *Journal of Micropalaeontology*, **37**, 431–443.

FLEISHER, R. L. 1974. Cenozoic planktonic foraminifera and biostratigraphy, Arabian Sea Deep Sea Drilling Project, Leg 23 A. *Initial Reports of the Deep Sea Drilling Project*, **23**, 1001–1072.

FOX, L. R. and WADE, B. S. 2013. Systematic taxonomy of early–middle Miocene planktonic foraminifera from the equatorial Pacific Ocean: Integrated Ocean Drilling Program, Site U1338. *Journal of Foraminiferal Research*, **43** (4), 374–405.

GAERTY, W. 2022. deeptime. https://github.com/willgearty/deeptime

GUILLOU, L., BACHAR, D., AUDIC, S., BASS, D., BERNEY, C., BITTNER, L., BOUTTE, C., BURGAUD, G., DE VARGAS, C., DECELLE, J., DEL CAMPO, J., DOLAN, J. R., DUNTHORN, M., EDVARDSEN, B., HOLZMANN, M., KOOISTRA, W. H. C. F., LARA, E., LE BESCOT, N., LOGARES, R., MAHÉ, F., MASSANA, R., MONTRESOR, M., MORARD, R., NOT, F., PAWLOWSKI, J., PROBERT, I., SAUVADET, A.-L., SIANO, R., STOECK, T., VAULOT, D., ZIMMERMANN, P. and CHRISTEN, R. 2013. The protist ribosomal reference database (PR^2): a catalog of unicellular eukaryote small sub-unit rRNA sequences with curated taxonomy. *Nucleic Acids Research*, **41**, 1–8.

HAMMER, Ø., HARPER, D. A. and RYAN, P. D. 2001. PAST: Paleontological statistics software package for education and data analysis. *Palaeontologia Electronica*, **4** (1), 4.

HECHT, A. D. 1974. Intraspecific variation in recent populations of *Globigerinoides ruber* and *Globigerinoides trilobus* and their application to paleoenvironmental analysis. *Journal of Paleontology*, **48**(6), 1217–1234.

HECHT, A. D. and SAVIN, S. M. 1972. Phenotypic variation and oxygen isotope ratios in Recent planktonic foraminifera. *Journal of Foraminiferal Research*, **2** (2), 55–67.

HEMLEBEN, C., SPINDLER, M., BREITINGER, I. and OTT, R. 1987. Morphological and physiological responses of *Globigerinoides sacculifer* (Brady) under varying laboratory conditions. *Marine Micropaleontology*, **12**, 305–324.

HEMLEBEN, C. and OLSSON, R. K. 2006. Wall textures of Eocene planktonic foraminifera. 47–66. *In* PEARSON, P. N., OLSSON, R. K., HUBER, B. T., HEMLEBEN, C. and BERGGREN, W. A. (eds) *Atlas of Eocene planktonic foraminifera*. Cushman Foundation of Foraminiferal Research, Special Publication, **41**.

HEMLEBEN, C., SPINDLER, M. and ANDERSON, O. R. 1989. *Modern planktonic foraminifera*. Springer-Verlag.

HSIANG, A. Y., BROMBACHER, A., RILLO, M. C., MLENECK-VAUTRAVERS, M. J., CONN, S., LORD-SMITH, S., JENTZEN, A., HENEHAN, M. J., METCALFE, B., FENTON, I., WADE, B. S., FOX, L., MEILLAND, J., DAVIS, C. V., BARANOWSKI, U., GROENEVELD, J., EDGAR, K. M., MOVELLAN, A., AZE, T., DOWSETT, H. J., MILLER, G., RIOS, N. and HULL, P. M. 2019. Endless forams: >34,000 modern planktonic foraminiferal images for taxonomic training and automated species recognition using convolutional neural networks. *Paleoceanography & Paleoclimatology*, **34**, 1157–1177.

HUBER, B. T., PETRIZZO, M. R., YOUNG, J. R., FALZONI, F., GILARDONI, S. E., BOWN, P. R. and WADE, B. S. 2016. Pforams@microtax: a new online taxonomic database for planktonic foraminifera. *Micropaleontology*, **62** (6), 429–438.

IACCARINO, S. and SALVATORINI, G. 1979. Planktonic foraminiferal biostratigraphy of Neogene and Quaternary of Site 398 of DSDP Leg 47B. *Initial Reports of the Deep Sea Drilling Project*, **47** (2), 255–285.

JENKINS, D. G., WHITTAKER, J. E. and CARLTON, R. 1986. On the age and correlation of the St. Erth Beds, SW England, based on planktonic foraminifera. *Journal of Micropalaeontology*, **5** (2), 93–105.

KEANY, J. and KENNETT, J. P. 1972. Pliocene-early Pleistocene paleoclimatic history recorded in Antarctic-Subantarctic deep-sea cores. *Deep Sea Research & Oceanographic Abstracts*, **19** (8), 529–548.

KENDALL, S., GRADSTEIN, F., JONES, C., LORD, O. T. and SCHMIDT, D. N. 2020. Ontogenetic disparity in early planktic foraminifers. *Journal of Micropalaeontology*, **39** (1), 27–39.

KENNETT, J. P. 1969. Distribution of planktonic foraminifera in surface sediments to the southeast of New Zealand. 307–322. *In* BRONNIMANN, P. and RENZ, H. H. (eds) *Proceedings of the First International Conference on Planktonic Microfossils, Geneva 1967*. Vol., **2**. EJ Brill.

KENNETT, J. P. and SRINIVASAN, M. S. 1983. *Neogene planktonic foraminifera: A phylogenetic atlas*. Hutchinson Ross, 265 pp.

KUCERA, M. and SCHÖNFELD, J. 2007. The origin of modern oceanic foraminiferal faunas and Neogene climate change. 409–425. *In* WILLIAMS, M., HAYWOOD, A. M., GREGORY, F. J. and SCHMIDT, D. N. (eds) *Deep-time perspectives on climate change: Marrying the signal from computer models and biological proxies*. Geological Society, London. The Micropalaeontological Society Special Publications.

LAM, A. R. and LECKIE, R. M. 2020. Late Neogene and Quaternary diversity and taxonomy of subtropical to temperate planktonic foraminifera across the Kuroshio Current Extension, northwest Pacific Ocean. *Micropaleontology*, **66** (3), 177–268.

LEROY, L. W. 1939. Some small Foraminifera, Ostracoda and Otoliths from the Neogene (Miocene) of the Rokan-Tapanoeli area, central Sumatra. *EurekaMag*, **1939**, 215–296.

LI, T., LIU, Z., HALL, M. A., BERNE, S., SAITO, Y., CANG, S. and CHENG, Z. 2001. Heinrich event imprints in the Okinawa Trough: evidence from oxygen isotope and planktonic foraminifera. *Palaeogeography, Palaeoclimatology, Palaeoecology*, **176** (1-4), 133–146.

MALMGREN, B. A. and KENNETT, J. P. 1977. Biometric differentiation between Recent *Globigerina bulloides* and *Globigerina falconensis* in the southern Indian Ocean. *Journal of Foraminiferal Research*, **7** (2), 131–148.

MALMGREN, B. A. and KENNETT, J. P. 1978. Test size variation in *Globigerina bulloides* in response to Quaternary palaeoceanographic changes. *Nature*, **275** (5676), 123–124.

MORARD, R., HASSENRÜCK, C., GRECO, M., FERNANDEZ-GUERRA, A., RIGAUD, S., DOUADY, C. J. and KUCERA, M. 2022. Renewal of planktonic foraminifera diversity after the Cretaceous Paleogene mass extinction by benthic colonizers. *Nature Communications*, **13** (1), 7135.

NAIDU, P. D. and MALMGREN, B. A. 1996. A high-resolution record of late Quaternary upwelling along the Oman Margin, Arabian Sea based on planktonic foraminifera. *Paleoceanography & Paleoclimatology*, **11** (1), 129–140.

OLSSON, R. K., BERGGREN, W. A., HEMLEBEN, C. and HUBER, B. T. 1999. *Atlas of Paleocene planktonic foraminifera*. Smithsonian Institution Press.

OLSSON, R. K., HEMLEBEN, C., HUBER, B. T. and BERGGREN, W. A. 2006. Taxonomy, biostratigraphy, and phylogeny of Eocene *Globigerina*, *Globoturborotalita*, *Subbotina*, and *Turborotalita*. 111–168. *In* PEARSON, P. N., OLSSON, R. K., HUBER, B. T., HEMLEBEN, C. and BERGGREN, W. A. (eds) *Atlas of Eocene planktonic foraminifera*. Cushman Foundation of Foraminiferal Research, Special Publication, **41**.

ORBIGNY, A. D. d' 1826. Tableau méthodique de la classe des Céphalopodes. *Annales des Sciences Naturelles*, **7**, 96–314.

ORBIGNY, A. d' 1846. *Foraminifères fossiles du bassin tertiaire de Vienne (Autriche)*. Gide & Comp.

OVECHKINA, M. N., BYLINSKAYA, M. E. and UKEN, R. 2010. Planktonic foraminiferal assemblage in surface sediments from the Thukela Shelf, South Africa. *African Invertebrates*, **51** (2), 231–254.

PARCERISA, D., GÀMEZ, D., GÓMEZ-GRAS, D., USERA, J., SIMÓ, J. A. and CARRERA, J. 2008. Estratigrafía y petrología del subsuelo precuaternario del sector SW de la depresión de Barcelona (Cadenas Costeras Catalanas, NE de Iberia). *Revista de la Sociedad Geológica de España*, **21**, 93–109.

PARKER, F. L. 1962. Planktonic foraminiferal species in Pacific sediments. *Micropaleontology*, **8** (2), 219–254.

PEARSON, P. N., OLSSON, R. K., HUBER, B. T., HEMLEBEN, C. and BERGGREN, W. A. 2006. *Atlas of Eocene planktonic foraminifera*. Cushman Foundation for Foraminiferal Research Special Publication, **41**, 513 pp.

POOLE, C. R. 2017. The late Neogene planktonic foraminifera genus *Globigerinoidesella*: taxonomy, biostratigraphy, evolution and palaeoecology. PhD thesis. University College London.

POOLE, C. R. and WADE, B. S. 2019. Systematic taxonomy of the *Trilobatus sacculifer* plexus and descendant *Globigerinoidesella fistulosa* (planktonic foraminifera). *Journal of Systematic Palaeontology*, **17** (23), 1989–2030.

POORE, R. Z. 1979. Oligocene through Quaternary planktonic foraminiferal biostratigraphy of the North Atlantic: DSDP Leg 49. *Initial Reports of the Deep Sea Drilling Project*, **49**, 447–517.

R CORE TEAM. 2013. R: a language and environment for statistical computing. R Foundation for Statistical Computing. https://www.R-project.org

REUSS, A. V. 1850. Neues Foraminiferen aus den schicten des Osterreichischen Tertiarbeckens. *Denkschriften der Akademie des Wissenschaften Wein*, **1**, 365–390.

SCHIEBEL, R. and HEMLEBEN, C. 2017. *Plankic foraminifers in the modern ocean*. Springer-Verlag, 358 pp.

SCHLITZER, R. 2022. Ocean data view. https://odv.awi.de/

SCHMIDT, D. N., CAROMEL, A. G. M., SEKI, O., RAE, J. W. B. and RENAUD, S. 2016. Morphological response of planktonic foraminifers to habitat modifications associated with the emergence of the Isthmus of Panama. *Marine Micropaleontology*, **128**, 28–38.

SCOTT, G. H. 2011. Holotypes in the taxonomy of planktonic foraminiferal morphospecies. *Marine Micropaleontology*, **78** (3–4), 96–100.

SICCHA, M. and KUCERA, M. 2017. ForCenS, a curated database of planktonic foraminifera census counts in marine surface sediment samples. *Scientific Data*, **4** (1), 1–12.

SOUSA, S. H. M., DE GODOI, S. S., AMARAL, P. G. C., VICENTE, T. M., MARTINS, M. V. A., SORANO, M. R. G. S. and MAHIQUES, M. M. 2014. Distribution of living planktonic foraminifera in relation to oceanic processes on the southeastern continental Brazilian margin (23–25°S and 40–44°W). *Continental Shelf Research*, **89**, 76–87.

SPEZZAFERRI, S. 1994. *Planktonic foraminiferal biostratigraphy and taxonomy of the Oligocene and lower Miocene in the oceanic record: An overview*. Palaeontographia Italica, **81**, 187 pp.

SPEZZAFERRI, S., OLSSON, R. K., HEMLEBEN, C., WADE, B. S. and COXALL, H. K. 2018. Taxonomy, biostratigraphy, and phylogeny of Oligocene and lower Miocene *Globoturborotalita*. 231–268. *In* WADE, B. S., OLSSON, R. K., PEARSON, P. N., HUBER, B. T. and BERGGREN, W. A. (eds) *Atlas of Oligocene planktonic foraminifera*. Cushman Foundation of Foraminiferal Research, Special Publication, **46**.

STEWART, I. A., DARLING, K. F., KROON, D., WADE, C. M. and TROELSTRA, S. R. 2001. Genotypic variability in subarctic Atlantic planktic foraminifera. *Marine Micropaleontology*, **43** (1–2), 143–153.

SRINIVASAN, M. S. 1975. Middle Miocene planktonic foraminifera from the Hut Bay Formation, Little Andaman Island, Bay of Bengal. *Micropaleontology*, **21** (2), 133–150.

SUCHARD, M. A., LEMEY, P., BAELE, G., AYRES, D. L., DRUMMOND, A. J. and RAMBAUT, A. 2018. Bayesian phylogenetic and phylodynamic data integration using BEAST 1.10. *Virus Evolution*, **4**, vey016.

THUNNELL, R. C. 1979. Mediterranean Neogene planktonic foraminiferal biostratigraphy; quantitative results from DSDP sites 125, 132 and 372. *Micropaleontology*, **25** (4), 412–437.

VAULOT, D. 2022. pr2database: PR2 database with shiny web interface. 2022. https://github.com/pr2database

VIOTTI, C. and MANSOUR, A. 1969. Tertiary planktonic foraminiferal zonation from the Nile Delta, U.A.R., Part II. *Globigerina nilotica*, a new species of foraminifera from the Miocene of the Nile Delta. 425–459. *In* SAID, R., BECKMANN, J. P., GHORAB, M. A., EL ANSARY, S., VIOTTI, C. and KERDANY, M. T. (eds) *Proceedings of the Third African Micropaleontological Colloquium, Cairo March 1968*. National Information and Documentation Centre, Cairo.

WADE, B. S., PEARSON, P. N., BERGGREN, W. A. and PÄLIKE, H. 2011. Review and revision of Cenozoic tropical planktonic foraminiferal biostratigraphy and calibration to the geomagnetic polarity and astronomical time scale. *Earth-Science Reviews*, **104** (1–3), 111–142.

WADE, B. S., OLSSON, R. K., PEARSON, P. N., HUBER, B. T. and BERGGREN, W. A. 2018. *Atlas of Oligocene planktonic foraminifera*. Cushman Foundation of Foraminiferal Research, Special Publication, **46**.

WANG, L. G., LAM, T. T. Y., XU, S., DAI, Z., ZHOU, L., FENG, T., GUO, P., DUNN, C. W., JONES, B. R. and BRADLEY, T. 2020. Treeio: an R package for phylogenetic tree input and output with richly annotated and associated data. *Molecular Biology & Evolution*, **37**, 599–603.

XU, X., YAMASAKI, M., ODA, M. and HONDA, M. C. 2005. Comparison of seasonal flux variations of planktonic foraminifera in sediment traps on both sides of the Ryukyu Islands, Japan. *Marine Micropaleontology*, **58** (1), 45–55.

YU, G., SMITH, D. K., ZHU, H., GUAN, Y. and LAM, T. T. Y. 2017. ggtree: an R package for visualization and annotation of phylogenetic trees with their covariates and other associated data. *Methods in Ecology & Evolution*, **8**, 28–36.